Progress in Organic Coatings 80 (2015) 156–163

Contents lists available at ScienceDirect

Progress in Organic Coatings

journal homepage: www.elsevier.com/locate/porgcoat

A forming limit curve for the corrosion resistance of coil-coatings based on electrochemical measurements

A.C. Bastos[a], G. Grundmeier[b], A.M.P. Simões[c,*]

[a] DEMaC and CICECO, University of Aveiro, 3810-193 Aveiro, Portugal
[b] Department of Technical and Macromolecular Chemistry, University of Paderborn, Warburger Str. 100, D-33098 Paderborn, Germany
[c] CQE and Department of Chemical Engineering, Instituto Superior Técnico, Universidade de Lisboa, Av. Rovisco Pais, 1049-001 Lisboa, Portugal

ARTICLE INFO

Article history:
Received 26 June 2014
Received in revised form
30 September 2014
Accepted 25 November 2014

Keywords:
Coil-coatings
Corrosion
EIS
FLC
Forming limit curve

ABSTRACT

Forming limit curves (FLCs) are useful tools to predict the safe forming limits of metal sheet. However, existing FLCs are limited to bare metal and the increasing use of pre-painted metal sheet (coil-coatings) requires new limits that take into account the corrosion resistance. In this work electrochemical impedance spectroscopy (EIS) was used to characterise the degradation of a coil-coated system in different states of deformation (uniaxial, biaxial and plane strain). The EIS data provided information about the condition of both paint and metal substrate and was used to devise criteria for minimum acceptable protection. A FLC was produced based on those criteria and its predictions were compared with the degradation of a model deep-drawn cup.

1. Introduction

Forming limit diagrams (FLDs) were initially developed by Keeler and Backhofen [1] and by Goodwin [2] in the 1960s. Until then the only reliable test of formability in metal sheet forming was the direct observation of whether or not the formed products were free of fracture and necking. FLDs became powerful tools providing an empirical gauge for forming limits. The key feature of a FLD is an experimentally determined forming limit curve (FLC), conventionally described as a curve in a plot of major strain vs minor strain – Fig. 1. The premise is that as long as the principal strains are significantly below this curve, the metal is safe from necking and tearing. Experimental methods for determining FLC are now well established [4–6].

The advent of pre-painted metal sheet (coil-coatings) brought a new problem to the field of limit prediction. In this material it is not just the metal sheet that is formed, but also the organic coating, as well as all other layers that may exist. Most commonly a coil-coating has a protective metallic layer (a thin layer of zinc or zinc alloys), pre-treatment (usually a brittle layer of phosphate) and various layers of paint (typically primer, mid-coat and top-coat). These layers have very different mechanical properties and respond differently to the same mechanical stress. It is difficult to predict the forming limits of a multilayer material like this. Moreover, the mechanical resistance is not the only matter of interest; corrosion resistance and aesthetics are also important, since this material is used as exterior cover of buildings and appliances.

In the present work a FLC was developed for the corrosion resistance of painted electrogalvanised steel. Samples of three different types of forming (uniaxial, biaxial and plane strain) were produced, with five degrees of deformation for each type. EIS was used to characterise the degradation of the paint layer and the corrosion of the metal substrate of each sample. Electrochemical parameters were used to estimate the limits of forming and, based on them, a FLC was constructed. The predictions given by the FLC were compared with EIS tests on model deep-drawn cups, which simulate real objects.

2. Experimental

2.1. Samples

The coil-coating used consisted of DC04 steel sheet 800 μm thick, with an electrodeposited zinc layer of 7 μm of nominal thickness and a phosphating pre-treatment. The paint scheme was composed by a 5 μm polyester primer plus a 15 μm polyurethane

* Corresponding author. Tel.: +351 218417963.
E-mail address: alda.simoes@tecnico.ulisboa.pt (A.M.P. Simões).

http://dx.doi.org/10.1016/j.porgcoat.2014.11.020
0300-9440/

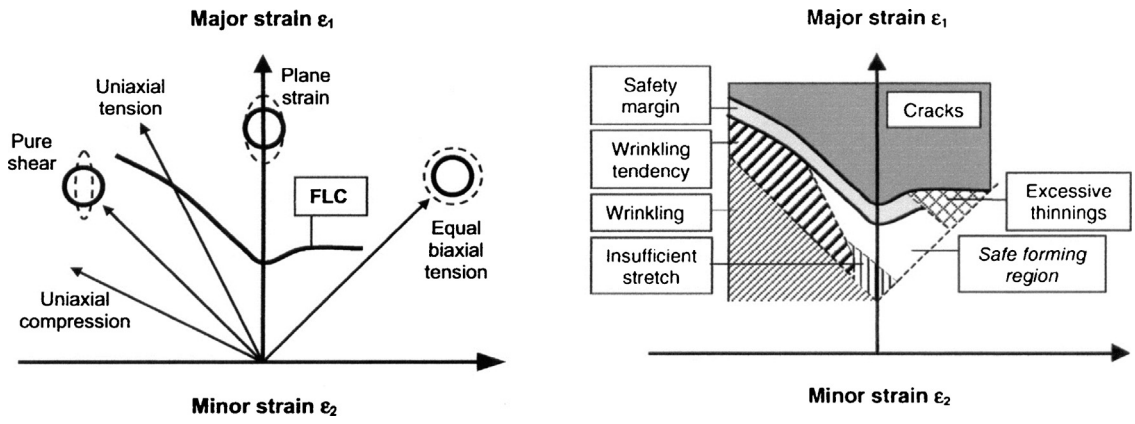

Fig. 1. Sketch of a forming limit curve, FLC and its corresponding forming limit diagram. Taken from Ref. [3] with permission.

mid-coat. To achieve faster degradation, no top-coat was used. Images of the different layers are shown in Fig. 2.

For the determination of the forming limit curve, samples with three types of mechanical deformation were produced – Fig. 3. Uniaxially strained samples (Fig. 3a) were produced by uniaxial traction. Plane strained (Fig. 3b) and biaxially strained (Fig. 3c) samples were produced by the Marciniak test. The strain was uniform in the flat top surface and only those regions were used for corrosion testing. For each type of deformation samples with five different levels of strain were produced. The major and minor logarithmic (or true) strains in each sample are presented in Table 1 and were determined by automated grid analysis with equipment and software from GOM mbH, Germany. A grid pattern of points was deposited on the surface of the unformed sheet and the deformation calculated by applying equation $\ln(l/l_0)$ in each principal direction, where l_0 and l are the distance between points before and after deformation, respectively.

Fig. 3d shows the model sample produced by deep drawing with the objective of testing the FLD. The strain distribution in this sample was also determined by automated grid analysis and is presented in Fig. 4.

2.2. Electrochemical impedance spectroscopy

Measurements were made on the flat area of the samples by exposing them to aqueous 5% (0.86 M) NaCl. A three-electrode arrangement was used, with a saturated calomel electrode as reference, a platinum counter electrode and the exposed sample area acting as working electrode. The cells were connected to Gamry (FAS1 Femtostat coupled to a PC4 controller board) or Solartron (1286 Electrochemical interface and HF 1255 frequency response analyser) instrumentation. All measurements were performed at room temperature, in a Faraday cage, with the solution quiescent and exposed to air. Impedance measurements were made at open

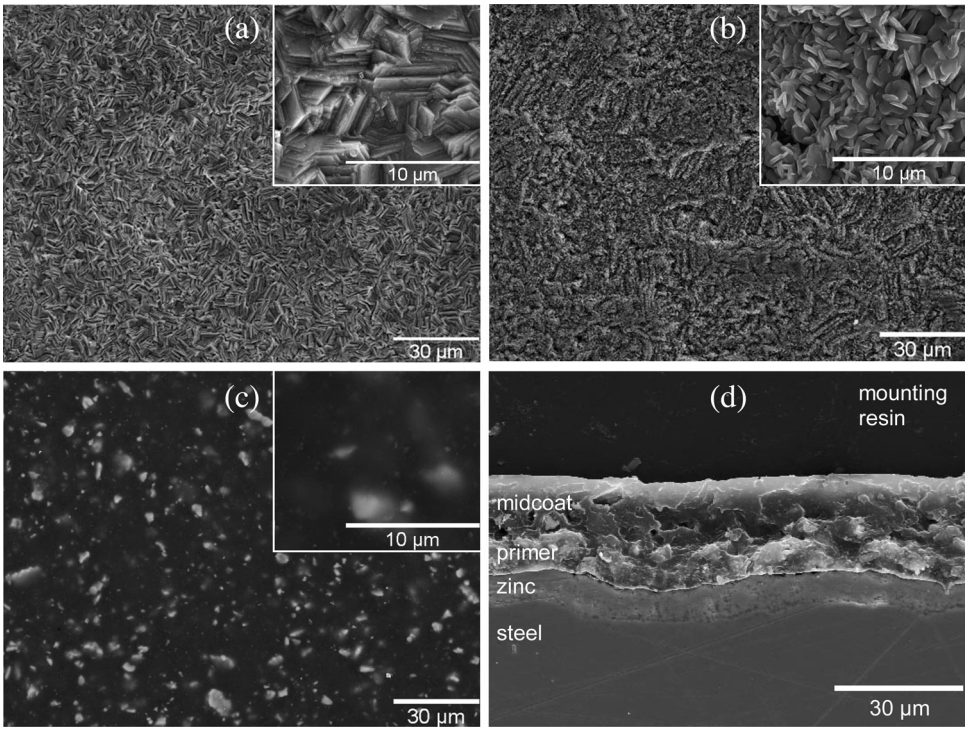

Fig. 2. Microscopic aspect of the different layers of the coil-coating: (a) electrogalvanised layer, (b) phosphate layer, (c) paint layer and (d) cross-section of the layered system.

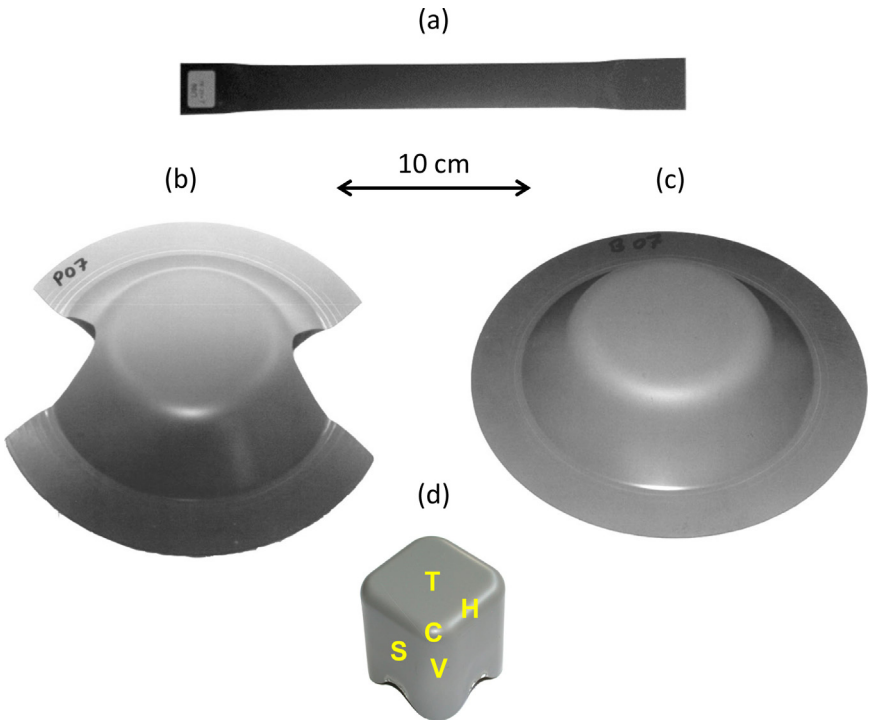

Fig. 3. Types of samples studied: (a) uniaxial strain, (b) plane strain, (c) biaxial strain and (d) model cup formed by rectangular deep-drawing (tested regions: T – top, H – horizontal edge, V – vertical edge, C – corner and S – side).

circuit potential, with a sinusoidal signal 10 mV rms, in the frequency range 50 kHz to ~5 mHz, with seven points per decade logarithmically distributed. A minimum of three samples were tested for each type of sample. Fitting of the spectra was made using ZView software from Scribner Associates (USA) or Boukamp's EQUIVCRT 4.55 [7,8].

3. Results

3.1. Construction of the FLC

Samples with five levels of strain of three distinct modes of deformation were exposed to 5% NaCl and monitored by EIS. Fig. 5 shows Bode plots of the impedance response of two samples, one with no strain and another with the highest strain tested (biaxial strain, $\varepsilon_1 = \varepsilon_2 = 0.1989$). These results are given as representative examples and a detailed analysis of the impedance of samples with uniaxial, biaxial and plane strain can be found in Refs. [9,10].

Usually, the impedance of painted metals [11–17] shows a single time constant at the beginning of immersion due to the response of the paint film, with the film capacitance (C_f) and the film resistance (R_f). A second time constant appears later, when corrosion starts at the paint–metal interface, with the response of the double layer capacitance (C_{dl}) and the charge transfer resistance (R_{ct}) at lower frequencies. These parameters can be used to follow the evolution of the protective properties of a painted system and rank the behaviour of a series of coatings. C_f measures the water absorption by the paint film, R_f is sensitive to the variation of its barrier properties, C_{dl} gives the coating delamination from the substrate and R_{ct} is an indication of the corrosion rate. A protective painted metal system should have low C_f, large R_f, absent or negligible C_{dl} and non-detected or high R_{ct}. In protective systems with a strong barrier effect these parameters present little variation with time. The results observed with the non-strained panels reveal an essentially capacitive behaviour in an initial stage and a gradual decrease in resistance at the low frequencies. Further, a second relaxation constant appearing at the low frequencies is associated with the corrosion process at the metal areas that have become exposed. The equivalent circuit used to describe the non-formed sample is present as inset in Fig. 5a.

In the case of the samples with strong deformation – case of Fig. 5b – the capacitance of the organic coating is observed only in the first day; then the drop of the coating resistance halts the detection of the coating capacitance in the analysed frequency range. Determination of the parameters from the experimental data was done by non-linear numerical fitting using electric equivalent

Table 1
Major ($\bar{\varepsilon}_1$) and minor ($\bar{\varepsilon}_2$) strains in each sample studied: three types of forming and five degrees of strain for each type.

Uniaxial			Biaxial			Plane		
ε/%[a]	$\bar{\varepsilon}_1$	$\bar{\varepsilon}_2$	mm[b]	$\bar{\varepsilon}_1$	$\bar{\varepsilon}_2$	mm[b]	$\bar{\varepsilon}_1$	$\bar{\varepsilon}_2$
0	0	0	0	0	0	0	0	0
9	0.0889	−0.4445	18	0.0488	0.0488	15	0.0564	0
11	0.1098	−0.0549	21	0.0770	0.0770	18	0.0770	0
16	0.1510	−0.0755	24	0.0917	0.0917	20	0.0953	0
19	0.1807	−0.0904	30	0.1484	0.1484	23	0.1310	0
23	0.2070	−0.1035	35	0.1989	0.1989	25	0.1570	0

[a] Elongation, $\varepsilon(\%) = [(l - l)/l_0] \times 100$ with l_0 and l distance between marks before and after deformation.
[b] Drawing depth of sample.

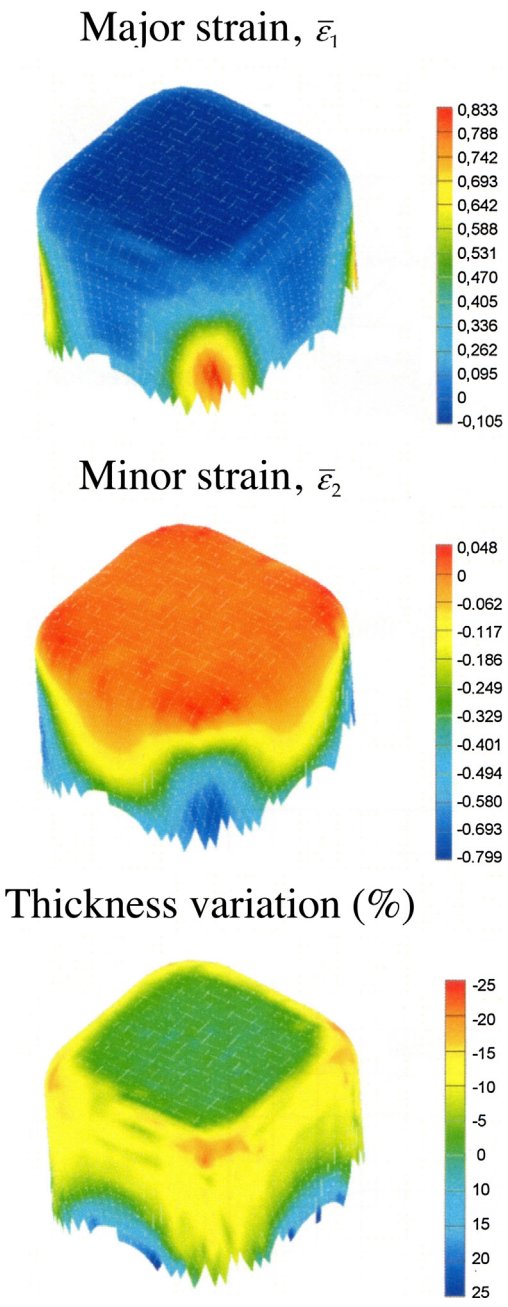

Fig. 4. Distribution of the major and minor strains and thickness variation on the deep-drawn cup.

circuits. Constant phase elements were used in the fitting procedure instead of pure capacitances, C, and for the purpose of comparison and ranking, it was considered to be acceptable the direct use of Y_0 ($F\,cm^{-2}\,s^{n-1}$) as an estimation of the capacitances ($F\,cm^{-2}$).

Fig. 6 shows the evolution of the parameters with time of immersion for a set of samples with uniaxial strain. Results for the three modes of deformation are reported in references [9,10]. $Y_{0,f}$ increased with time up to a plateau. Then, after some time, and starting from the most strained samples, a sudden increase was observed. R_f was very high at the instant of immersion, decreasing rapidly in the first 10 days and in a smoother way afterwards. Until 16% the drop was clearly dependent on the degree of elongation, then, up to 23%, the influence of strain was negligible. The first signs of corrosion were observed when R_f was below 10^7–$10^8\,\Omega\,cm^2$. The time for corrosion initiation, taken as time for detection of the double layer capacitance, decreased with increasing strain. The double layer capacitance increased with the elongation between 9% and 19% and no further increase was observed for 23%. R_{ct} appeared in the spectra at the same time as C_{dl} with high values that decreased in time, following a trend inverse to the observed for C_{dl}. When analysing Fig. 6 it becomes clear that the most strained samples presented the lowest resistances, the highest capacitances and the fastest parameter changes, all characteristics of fast degradation.

3.2. Testing of the FLC

To test the predictions of the FLC, deep-drawn cups with different strained regions were produced in order to mimic real objects. The overall degradation of the cup and of five distinct regions (top, corners, sides, vertical and horizontal edges) was analysed by EIS and the results reported elsewhere [18,19]. Here just a brief account is presented. As shown in Fig. 7, the impedance of the whole cup was already low just 1 h after immersion and dropped rapidly with the time of immersion. The regions of the cup have distinct impedance response as a reflection of the different protective properties which in turn are related to the strain distribution along the cup. Fig. 8 gives the variation of the impedance parameters obtained by fitting the experimental data. Only the top shows good corrosion resistance. This is confirmed by visual inspection of the cups. Blisters appeared at the corners just after 1 day of immersion and by the end of the testing period all regions except the top had many blisters, large and prominent – Fig. 9.

4. Discussion

4.1. Determination of limits for safe forming

To establish forming limit curves accounting for the anticorrosion performance, methodology and criteria different from that used to determine traditional FLCs are required. The best choice might be the exposure to service conditions but this is time consuming and many years are needed for obtaining useful data. Short-term tests are normally preferred, which brings the problem of their reliability to predict long-term performance. The Corrosion Committee of the Federation of Societies for coatings technology considered a short-term test as consisting of four basic components [20]:

- *Specimens preparation*. This includes the even substrate preparation, proper coating application, uniform and accurate film thickness, correct conditioning and adequate number of specimens.
- *Induction of degradation*. Conditions chosen to cause the short-term degradation.
- *Evaluation of the degradation*. Methods and techniques used to assess the level of degradation.
- *Analysis of the data*. Ways used to treat the experimental data in order to predict the long-term performance of the protective coating system.

All four components are critical to guarantee the quality and representativeness of the test. In this work the paint application and the forming processes were made under strict quality control and a minimum of three samples was tested for each deformation state. The other components are now discussed.

4.1.1. Testing environment

Continuous immersion in 5% NaCl was used as exposure medium, a choice based on the need for fast degradation. NaCl aqueous solutions are the most common environment used in corrosion

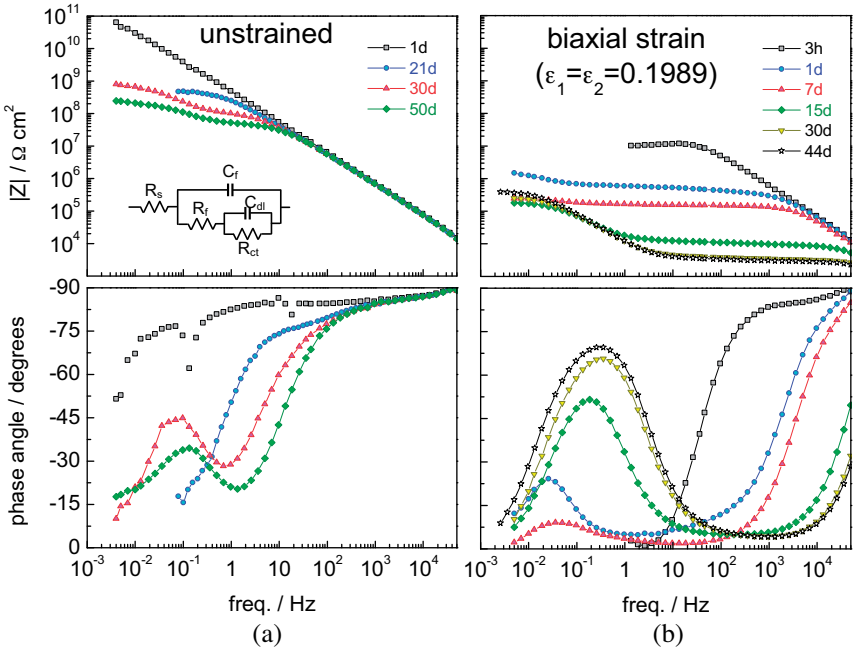

Fig. 5. Bode plots of an unstrained panel (a) and of biaxially strained to a drawing depth of 35 mm, $\varepsilon_1 = \varepsilon_2 = 0.1989$ (b).

laboratories for electrochemical testing of painted metals [21]. Still, some questions may be raised on such test conditions that seem more appropriated for paints used in marine environments, not for systems to be used in architecture, appliances or automotive parts. If the accelerated test ranks the samples in the same way as in real exposure, then it will certainly be suitable, although it is still necessary to find the correlation between the times of degradation in immersion and in service.

4.1.2. Evaluation of degradation

The evaluation of samples degradation was done by EIS. This technique provides quantitative parameters that can be related to different aspects of the system's performance (paint degradation and corrosion of the metal substrate) [11–17] and be used to determine limit values of acceptable performance. A brief discussion regarding the use of each parameter is now presented.

a) *Film capacitance, C_f.* Water can become distributed throughout the paint film in a continuous and homogeneous way but it may also exist in points of preferential accumulation, like hydrophilic components of the paint, voids, in blisters and at the substrate–paint interface. Galvan et al. [22] elected this parameter as the best indicator of coating performance. For these authors the paint film capacitance has the advantage of being

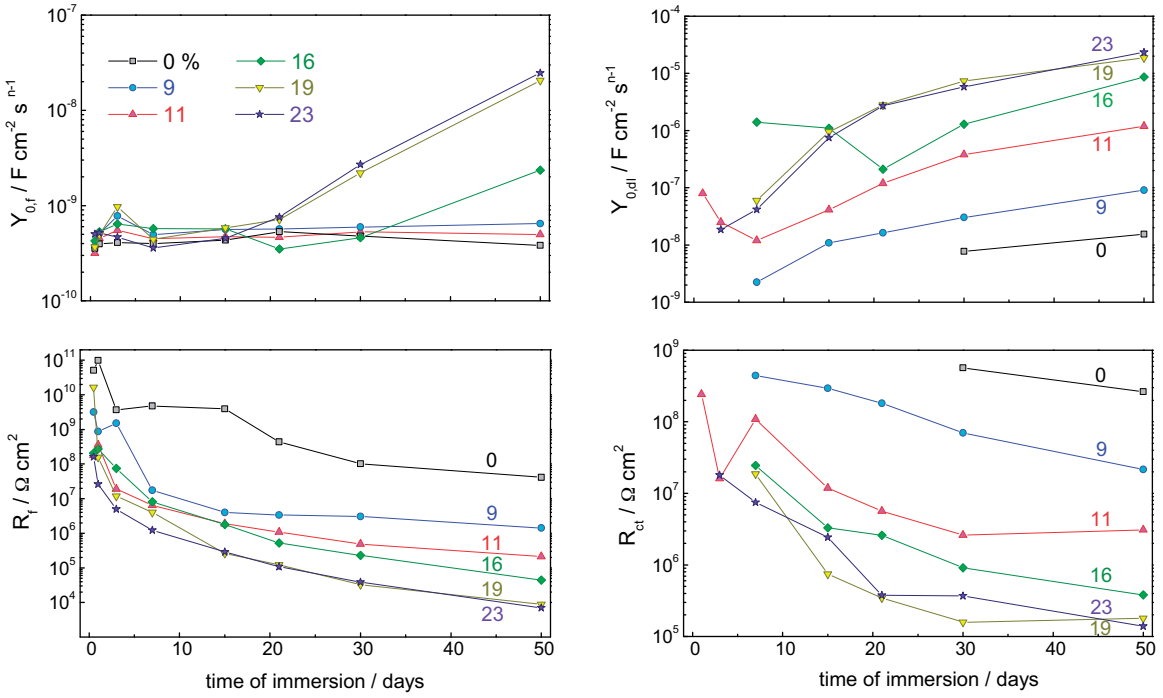

Fig. 6. Evolution with time of immersion of the parameters $Y_{0,f}$, R_f, $Y_{0,dl}$, R_{ct} of a set of uniaxially strained samples. Elongation (%) is indicated in the graph.

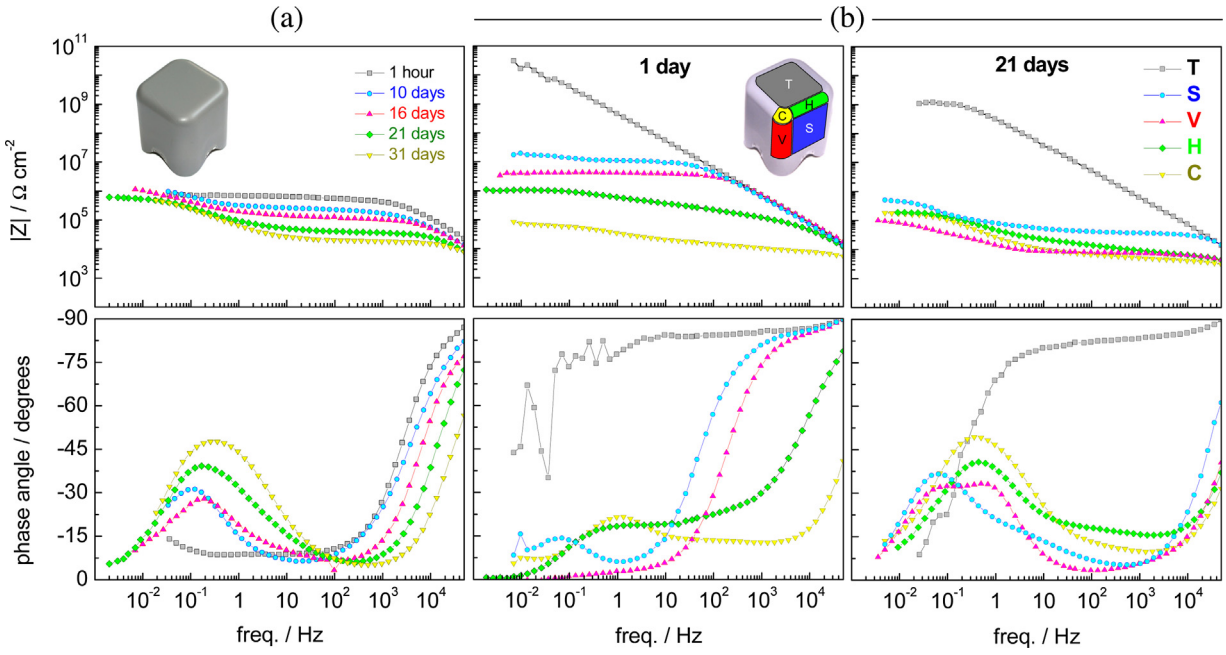

Fig. 7. Impedance response of (a) whole deep-drawn cup and (b) five regions of the cup.

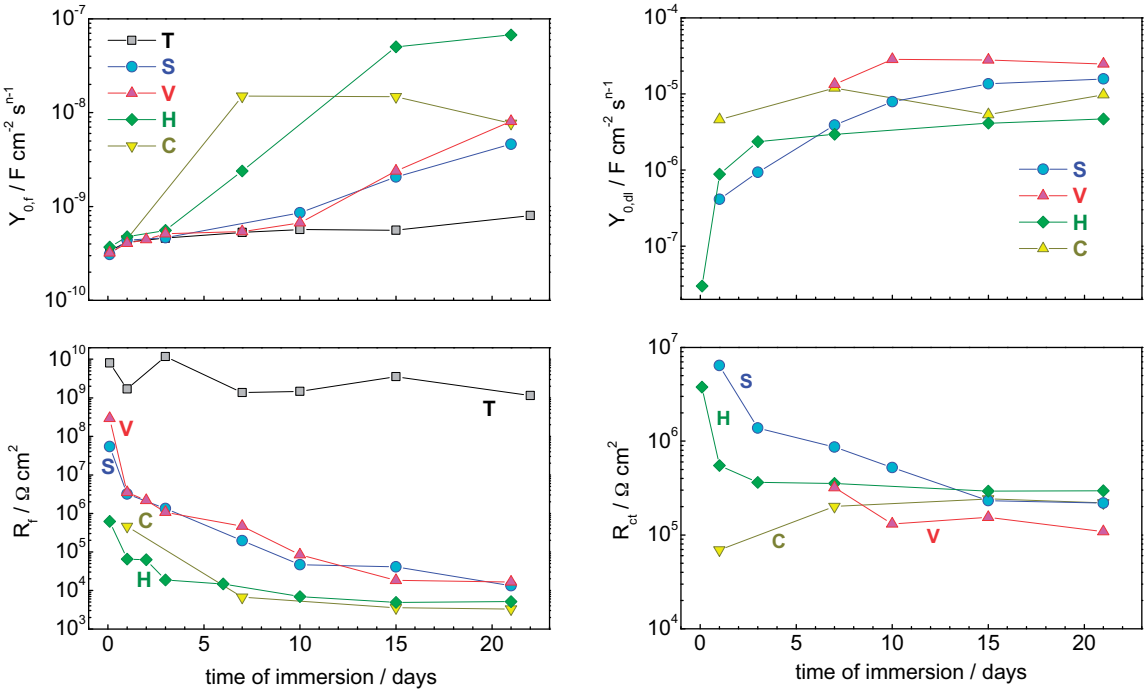

Fig. 8. Evolution with time of immersion of the parameters $Y_{0,f}$, R_f, $Y_{0,dl}$, R_{ct} of each region of the cup.

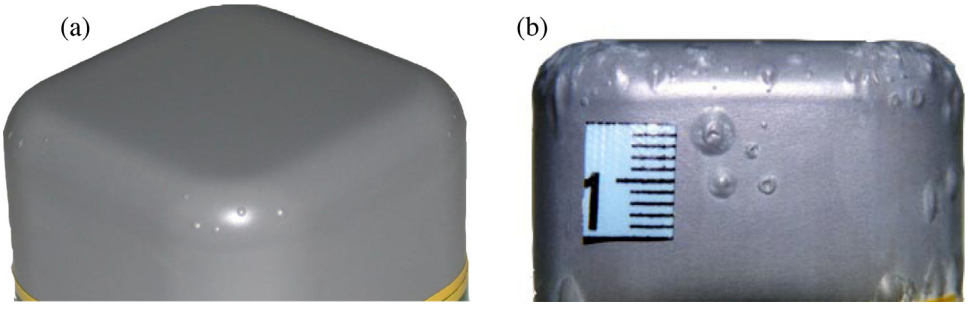

Fig. 9. Cup degradation after (a) 1 day and (b) 22 days of immersion.

measurable throughout the test period and reflects the deterioration at a microscopic scale in numerous points of the paint. They also considered this parameter as the most reproducible of all passive elements of the system. Conversely, for Walter [23], this parameter must not be used to estimate the paint degradation because after some time of immersion it attains a stable plateau while the system continues to deteriorate. On the other hand, other authors identified a moment in C_f evolution when, after a period of stability, a marked rise occurs [24]. This can be observed in Fig. 6a. That moment was denominated *coating breaking point*, and considered to be the time when the system loses its protective capabilities. In fact, when this happens, C_f is no longer measured. A significant amount of water absorbed by the paint or at the metal–paint interface, or even a layer of corrosion products, is measured instead. Advantages of C_f are the detection since the beginning of immersion and its response at high frequencies, meaning that the measurements can be made fast. A disadvantage is the risk of no correlation between the initial water uptake and the anticorrosive performance of the paint system.

b) *Film resistance*, R_f. In our work [9,10,18,19] this proved to be the most reliable parameter to evaluate the degradation of painted metals, being sensitive to the effects of mechanical deformation and showing a regular evolution with the time of immersion. It correlated well with the macroscopic and microscopic degradation of the samples. Usually R_f can be measured throughout the testing period and gives information about the barrier properties of the organic coating to ionic transport. Limiting cases can occur when R_f is not detected. In very protective systems, the response is capacitive and R_f is detected just after the decrease of the total impedance. Some systems described in the literature [25–27] showed only a capacitive response and very high impedance even when intense corrosion was detected in the metal substrate. In these cases EIS is unable to describe the system degradation correctly. Another limiting case occurs when the paint film is so porous or so degraded that R_f cannot be distinguished from R_s.

c) *Double layer capacitance*, C_{dl}. This parameter is normally absent on protective systems. The beginning of its detection occurs with the initiation of the electrochemical activity of the metal substrate. Thus, C_{dl} appears after film degradation or when defects exist. No information is given about the paint film except its delamination from the substrate. For that, it is assumed that the nature of the double layer does not change from bare to coated metals and that any increment in C_{dl} will be caused by a proportional increase in the wetted area under the coating. However, corrosion products and adsorbed species may also contribute to the measured capacitance.

d) *Charge transfer resistance*, R_{ct}. Like for the double layer capacitance, this parameter is not detected on protective systems and needs some degradation or defects to manifest. It is inversely proportional to the corrosion rate [11]. R_{ct} may also be used to estimate delamination by comparing its value with the one measured on the uncoated substrate. This is valid provided the change is caused only by the increase in exposed area. It must be noted that C_{dl} and R_{ct} depend on the metal surface condition, which can be altered by changes of local pH, dissolved oxygen or metal cation concentration that normally occur in the course of the corrosion process.

In summary, EIS parameters are able to characterise the system in terms of water uptake, barrier properties, delamination and corrosion rate. Depending on the celerity and reliability desired, a single parameter or a set of parameters may be used.

Table 2
Possible criteria for forming limit acceptance.

Parameters	1 day	3 days	30 days
$Y_{0,f}$ ($F\,cm^{-2}\,s^{n-1}$)	$<10^{-9}$	$<10^{-9}$	$<10^{-9}$
R_f ($\Omega\,cm^2$)	$>10^9$	$>10^8$	$>10^6$
$Y_{0,dl}$ ($F\,cm^{-2}\,s^{n-1}$)	Absent	$<10^{-8}$	$<10^{-7}$
R_{ct} ($\Omega\,cm^2$)	Absent	$>10^7$	$>10^6$

4.1.3. Criteria for estimating limits of performance

For each parameter it is necessary to identify the threshold values beyond which damage is not acceptable. The lower the C_f the better, but often values smaller than $10^{-9}\,F\,cm^{-2}$ represent low water absorption. A value of $R_f = 10^6\,\Omega\,cm^2$ has been considered to be the point below which underpaint activity is detected by EIS [12] but, in this work, activity at the surface was observed for R_f values of 10^7–$10^8\,\Omega\,cm^2$ [9,10]. Typical values of C_{dl} for a bare metal are 10–50 $\mu F\,cm^{-2}$, and in that case values of $10^{-7}\,F\,cm^{-2}$ represent ~1% of delaminated area, which seems to be a fair limit of protection. For R_{ct} the higher the value the better. Using the same 1% delamination criterion and considering a R_{ct} of the substrate of 10^3–$10^4\,\Omega\,cm^2$, values of 10^5–$10^6\,\Omega\,cm^2$ can be considered the threshold limit.

Based on these considerations, possible criteria are advanced in Table 2. The results obtained in the first day of testing are of particular interest due to the rapid assess of data but it since some of the elements of the equivalent circuit may not be measurable in the first stage, it is advisable to wait more time to confirm the behaviour suggested at the beginning of immersion. These criteria have just the intention of illustrate how the experimental results can be used. Their validity relies on the correspondence with real exposure.

From Table 2 it is possible to define the maximum acceptable deformation. Uniaxial strained samples in Fig. 7 satisfy all criteria until 9% of elongation. Depending on how strict Table 2 is taken into consideration, it may or may not be safe to strain the material up to 11% of elongation, since some criteria, but not all, are met. Similar analysis for biaxially strained samples gives accepted deformation for drawing depths of 18 mm but not for 21 mm. For plane strain, drawing depths of 18 mm are acceptable but not 20 mm.

In a previous paper [10] the three types of strain, uniaxial, plane and biaxial, were compared using the equivalent plastic strain, a parameter that reflects the overall strain in a sample, allowing the direct comparison of samples with different types of deformation. Applying the criteria in Table 2 leads to an equivalent plastic strain of 0.10–0.15 as forming limit.

4.2. Construction of a forming limit diagram

In Fig. 10 the *Y* and *X* axis correspond to the major and minor strains, respectively. Points corresponding to the tested samples are

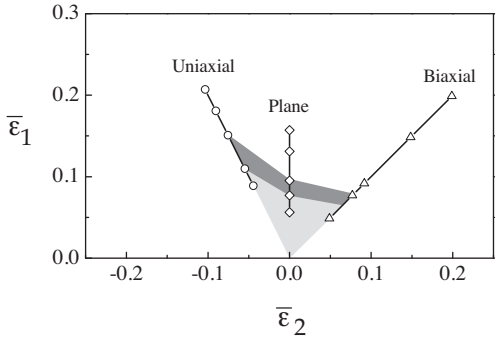

Fig. 10. Forming limit curve based on the criteria in Table 2 and on electrochemical tests with uniaxial, biaxial and plane strained samples.

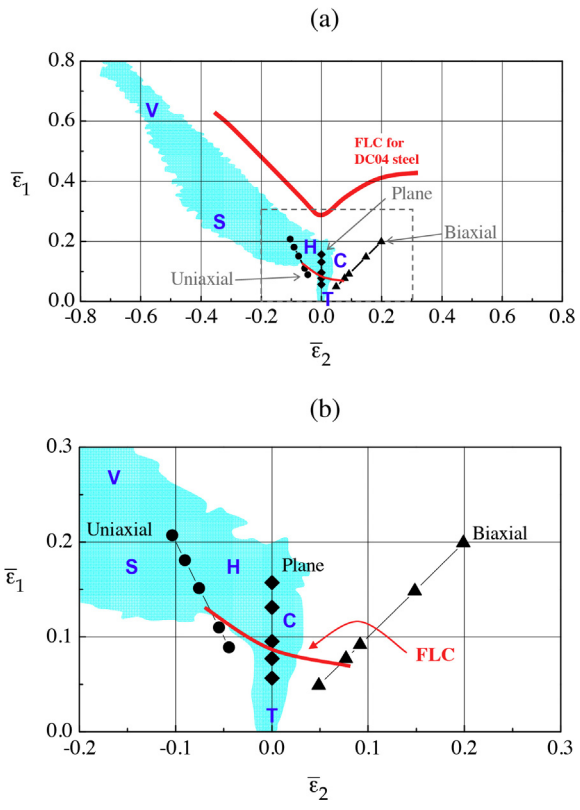

Fig. 11. (a) FLD to predict the corrosion resistance of the deep-drawn cup. The strain distribution in the cup and a forming limit curve for DC04 steel sheet are included. (b) Expansion of the region delimited by dashed line.

placed in the diagram according to their forming states (Table 1). Using the criteria in Table 2, the grey band separates the region of acceptable forming from the region where degradation is not admissible, i.e., separates the samples that meet the criteria from those that do not. The FLC lies inside the grey band.

The limits for corrosion resistance are lower than the limits for the structural function of the DC04 steel sheet, shown in Fig. 11. This means that a single FLC is not satisfactory when more than one property is important. In coil-coatings, different limits may exist for properties as diverse as mechanical resistance, corrosion resistance or gloss.

The quality of this FLC depends on its reliability to predict the behaviour of the material in real service. Extrapolation to other systems must be made with caution. A great variety of coil-coatings exist, with different base metals, metallic coatings, pre-treatments and paint schemes. Paints based on polymers with different mechanical behaviour and different pigmentation (pigment type, size, shape and pigment volume concentration) will give different corrosion resistance for the same forming state.

4.3. Comparison of the FLD predictions with the performance of a deep-drawn cup

The forming limit diagram was tested comparing its predictions with the results obtained in selected regions of the deep drawn cup. Fig. 11 depicts the major and minor strains on the cup with the approximate position of each region, together with the FLC for DC04 steel and the FLC developed for corrosion resistance. This new FLC is positioned at much lower values of major strain. According to the FLD, the only region fully inside the safe region is the top of the sample, region T. All other regions are above the FLC, which leads to the prediction of high degradation and fast corrosion. This is clearly consistent with what was experimentally found by EIS and visual inspection. The corner was the first region to show signs of degradation, with very low impedance and blisters appearing in the first day of immersion. Regions V, H and S had moderate degradation, whereas the top side remained undamaged during the testing period. The consequences of the strain on this multi-layer material are of diverse nature. Apart from residual stresses that may endure on the paint layer and the possible loss of adhesion at some points, cracking of the phosphate layer was observed as well as microscopic holes on the surface of the most strained regions [19]. The reduction of the paint film thickness was also observed and, according to Fig. 4, the corner suffered the highest thickness reduction (up to 25%).

5. Conclusions

A forming limit curve for the corrosion resistance of a coil-coating was obtained based on electrochemical parameters. The limitations of the methodology were discussed, in particular the criteria used to estimate the limits of safe forming. The FLC was tested with the response of a deep-drawn cup and good correlation was observed between the prediction and the degradation in different regions of the cup. Extrapolation to other systems must be done with care since coil-coatings are multi-layered systems with many possible combinations of layers with distinct characteristics.

Acknowledgements

The authors acknowledge funding from ECSC/RFCS under contact no. 7210-PR/189. They also thank L. Engl (Thyssen Krupp Stahl, Dortmund, Germany) for the materials and samples used.

References

[1] S.P. Keeler, W.A. Backhofen, ASM Trans. Quart. 56 (1964) 25.
[2] G.M. Goodwin, SAE Paper 680093, 1968.
[3] S. Holmberg, B. Enquist, P. Thilderkvist, J. Mater. Process. Technol. 145 (2004) 72.
[4] T.B. Stoughton, Int. J. Mech. Sci. 42 (2000) 1.
[5] T.B. Stoughton, X. Zhu, Int. J. Plast. 20 (2004) 1463.
[6] H. Yao, J. Cao, Int. J. Plast. 18 (2002) 1013.
[7] B.A. Boukamp, Solid State Ionics 18–19 (1986) 136.
[8] B.A. Boukamp, Solid State Ionics 20 (1986) 31.
[9] A.C. Bastos, A.M.P. Simões, Prog. Org. Coat. 46 (2003) 220.
[10] A.C. Bastos, C. Ostwald, L. Engl, G. Grundmeier, A.M. Simões, Electrochim. Acta 49 (2004) 3947.
[11] A. Amirudin, D. Thierry, Prog. Org. Coat. 26 (1995) 1.
[12] M. Kendig, J. Scully, Corrosion 46 (1990) 22.
[13] J. Titz, G.H. Wagner, H. Spähn, M. Ebert, K. Jüttner, W.J. Lorenz, Corrosion 46 (1990) 221.
[14] F. Mansfeld, J. Appl. Electrochem. 25 (1995) 187.
[15] F. Mansfeld, M.W. Kending, S. Tsai, Corrosion 38 (1982) 478.
[16] P.L. Bonora, F. Deflorian, L. Fedrizzi, Electrochim. Acta 41 (1996) 1073.
[17] G. Grundmeier, A. Simões, Corrosion protection by organic coatings, in: A.J. Bard, M. Stratmann (Eds.), Encyclopedia of Electrochemistry, vol. 4, Wiley-VCH, Weinheim, 2003, pp. 499–565.
[18] A.C. Bastos, A.M.P. Simões, Prog. Org. Coat. 65 (2009) 295.
[19] A.C. Bastos, M.G.S. Ferreira, A.M.P. Simões, Electrochim. Acta 56 (2011) 7825.
[20] B.R. Appleman, J. Coat. Technol. 62 (1990) 57.
[21] J.N. Murray, Prog. Org. Coat. 30 (1997) 225.
[22] J.C. Galvan, S. Feliu, M. Morcillo, Prog. Org. Coat. 17 (1989) 135.
[23] G.W. Walter, Corros. Sci. 32 (1991) 1041.
[24] D.M. Brasher, J.T. Nurse, J. Appl. Chem. 9 (1959) 96.
[25] M.C. Bernard, S. Duval, S. Joiret, M. Keddam, F. Ropital, H. Takenouti, Prog. Org. Coat. 45 (2002) 399.
[26] E. Spengler, F.L. Fragata, I.C.P. Margarit, O.R. Mattos, Prog. Org. Coat. 30 (1997) 51.
[27] I.C.P. Margarit, O.R. Mattos, Electrochim. Acta 44 (1998) 363.